Formation of chain and V-shaped structures in the initial stage growth of Si/Si(100)

Shudun Liu, C. S. Jayanthi, and Shi-Yu Wu
Department of Physics, University of Louisville, Louisville, Kentucky 40292

Xiaorong Qin
University of Wisconsin-Madison, Madison, Wisconsin 53706

Zhenyu Zhang
Solid State Division, Oak Ridge National Laboratory, Oak Ridge, Tennessee 37831-6032

Max G. Lagally
University of Wisconsin-Madison, Madison, Wisconsin 53706

(Received 25 November 1998; revised manuscript received 2 August 1999)

New growth structures (chain and V-shaped structures) have recently been observed in scanning tunneling microscopy studies of Si and Ge adatoms deposited on Si(100). We have studied the basic building block, the nature and the formation of these growth structures by using a combination of theoretical techniques including the O(N) nonorthogonal tight-binding molecular dynamics and local analysis of the electronic structure. We find that the interplay between the binding energy, diffusion barrier, and temperature is the key to the formation of these structures.

Thin film growth of semiconductor materials is a highly nonequilibrium process where the kinetics of growth plays a crucial role in determining the growth structures. An understanding of all relevant mechanisms influencing the growth at the microscopic level is particularly important because of the current trend towards nanoscale fabrication of devices. Despite the strides made in thin film semiconductor technology, much remains to be understood on nucleation and epitaxial growth mechanisms at a fundamental level. Many critical issues regarding the nature and the sizes of the stable nuclei for growth on Si(100) still remain open. For a better understanding of the thin film growth, recent theoretical and experimental investigations have focused their attention on studies of the early stages of growth.[1–8]

In the initial stages of growth corresponding to low coverages of adatoms, scanning tunneling microscopy (STM) experiments of Si/Si(100),[5] Ge/Si(100),[6] and Si/Ge(100) (Ref. 7) have revealed a new type of growth structure near room temperature. This growth structure appears as a chain of ''adatom units'' with the chain intersecting the substrate dimer rows obliquely at a specific angle. These ''adatom units'' are located in the trough of the substrate. These structures are abundant and stable near room temperature. They are structurally different from the previously found dilute-dimer rows, which intersect the substrate dimer rows at a right angle. Furthermore, the dilute-dimer row structure is predominantly observed above room temperature ($\sim$400 K). Most importantly, the chain and the dilute-dimer-row structures behave very differently when the polarity of the bias voltage is reversed in the STM experiment. The chain structure is found to be faint in the filled-state image and bright in the empty-state image, similar to the behavior of monomers on the Si(100) substrate. In contrast, the dilute-dimer-row is found to be bright in both situations. Based on this experimental result, Qin and Lagally[6] had suggested that the basic building unit of the chain structure is, perhaps, not a dimer, but a pair of atoms. This would also imply that dilute-dimer-row and chain structures, in addition to being structurally different, are also electronically different entities. In addition to the chain structure, V-shaped structures have also been observed for Si/Si(100) (Ref. 5) at room temperatures and low coverages.

In this communication, we aim to understand (i) the nature of the basic-building unit of the chain and V-shaped structures, namely, whether they are dimers or a pair of atoms, (ii) the bias dependence of the STM images of these structures, and (iii) conditions for the formation of these structures in the initial stage of growth of Si/Si(100).

The modeling of the low coverages ($\sim$0.01 ML) of Si/Si(100) in the study of the initial stage of growth requires a large surface cell. This requirement makes the total energy and force calculations rather expensive using first-principles molecular dynamics (MD) schemes. On the other hand, tight-binding based MD can handle larger systems than *ab initio* MD, while, at the same time, incorporating explicitly the quantum mechanical description of electrons.[9,10] In this work, we employ an order-$N(O(N))$ MD scheme based on a nonorthogonal tight-binding (NOTB) Hamiltonian.[11]

Slab models of appropriate sizes for the different geometries of the reconstructed surfaces of Si(100) are first set up. The sizes of the slab are chosen so as to ensure that finite size effects such as image-image interactions are small. Typical sizes used in our calculations range from 4×4 to 8×8 in the lateral direction and from 12 to 24 layers in the z direction. The bottom of the slab (2–4 layers) are fixed at their bulk positions as determined by the NOTB-MD ($a=5.46$ Å), while the rest of the system (including adatoms, if any) are fully relaxed. The total energy of the slab calculated via the NOTB Hamiltonian of Menon and Subbaswamy[12] is minimized using the molecular dynamics-

based annealing and quenching techniques. Typically, a simulation is stopped when the energy fluctuation is less than 0.01 eV over 100 time steps. In our calculations, we found the correct trend for the ordering as well as values of surface energies for all the commonly studied reconstructed surfaces of Si(100).[13–15] For example, the surface energies of the 1×1 relaxed, 2×1 symmetric, 2×1 asymmetric, $p2\times2$, and $c4\times2$ structures were found lower than the bulk-terminated case by the following amounts: 0.02, 0.93, 0.96, 1.0, and 1.01 eV/atom, respectively. Furthermore, the buckling angle of the tilted dimers on the $c4\times2$ reconstructed surface is found to be 16.9 degrees, which also agrees very well with the *ab initio* result of 17.5 degrees.[15] The bond length of the dimer on the $c4\times2$ surface is found to be 2.38 Å, which is somewhat larger than the *ab initio* result of 2.29 Å.[15] The experimental measurements of the dimer bond length are inconclusive so far, suggesting a value between 2.20 and 2.45 Å.[16–18]

Although the NOTB Hamiltonian of Menon and Subbaswamy[12] predicts the correct structural properties for Si(100), it does not yield the correct charge transfer from the lower atom of a buckled dimer to the upper atom. It predicts a charge transfer of about $0.8e$ which is much larger than the experimental estimate of $0.33e$.[19] To correct for this excess charge transfer, we have incorporated an on-site Hubbard term which is given by $U(Q_i-Z_i)$, where Q_i is the valence electronic charge associated with site i, and Z_i is the total charge associated with the valence electrons of an isolated Si atom ($Z_i=4$). In our calculations, we have chosen $U=3$ eV, a reasonable value based on a previous tight binding study of Si(111).[20] The modified NOTB Hamiltonian yields a charge transfer of $0.3e$, in good agreement with the experiment. Although the reduction of charge transfer affects the local binding energy, we found that the surface energy changes by an amount less than 0.01 eV/atom. Therefore, this does not lead to any changes in the reconstructed structures of clean Si(100).

The modified NOTB Hamiltonian was used in our subsequent studies on the adsorption of Si adatoms on the Si(100) surface. A self-consistent calculation is performed at each MD step until fluctuations of charges are less than $10^{-6}e$ per atom. The adsorption of a monomer on Si(100) has been studied extensively in the past.[21–24] The global minimum and various local minima have been carefully examined.[21,23] In our MD simulations, we found that for a monomer, the most favorable adsorption site is situated between the dimer rows of the $c4\times2$ structure and on top of a second layer atom, referred usually as *M* site (e.g., see Ref. 22). This result is in agreement with both the experiment[2] and *ab initio* results.[21,23,24]

We next performed MD simulations for two silicon adatoms placed in the trough between the substrate dimers of the $c4\times2$ surface of Si(100). It is known from the experiment that the adsorption of such an ''adatom pair'' breaks the symmetry of the underlying substrate by interrupting the ''antiferromagnetic'' buckling of the dimer rows on which the adatoms reside.[5] To accommodate this reconstruction and to allow for the relaxation of substrate atoms in the vicinity of the adatom unit, a large surface unit cell must be used in the calculation. In our MD simulations, we used a slab of size $8\times8\times12$. The size of the simulation cell used in our calculation is larger than those used in recent studies of similar systems.[10,15,22–24] Figure 1 shows the results of our MD simulation for two adatoms placed in the trough. In this figure the break in $c4\times2$ symmetry and the rearrangement of substrate atoms for the dimer rows flanking the adatoms can be seen. Our simulation yields the equilibrium separation between the adatoms to be 2.52 Å. Since this separation is close in value to the equilibrium distance of an isolated Si dimer, it suggests that the two adatoms in the trough are chemically bonded.

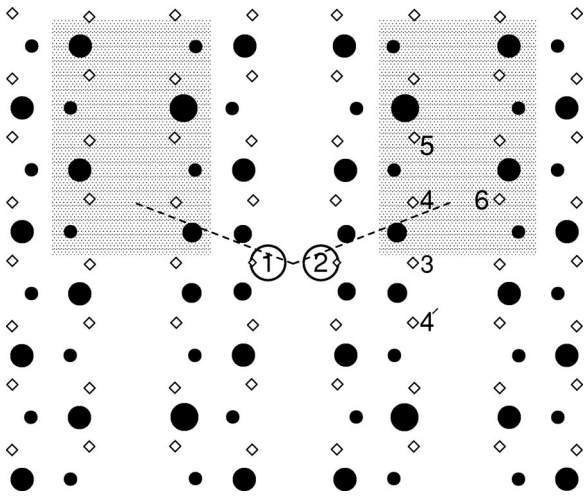

FIG. 1. Top view of Si(100) surface with a ''pair of adatoms'' in the trough (*C* dimer). Open circles: adatoms. Solid circles: top layer substrate atoms. Diamonds: second layer atoms. Atoms denoted by larger symbols are higher than those by smaller ones. The antiferromagnetic buckling of the $c(4\times2)$ in the middle two rows is interrupted by the adsorption of adatoms. Locations marked as 3, 4, and 5 are the three tested positions of the third adatom as discussed in the text. The growth direction of the chain structure is indicated by the line connecting the pairs of atoms ''1–2'' and ''4–6,'' respectively. The V-shaped structure is indicated by the pair of lines in the figure.

We examined the bond charge between the two adatoms by performing a local analysis of the electronic structure using a method akin to Mulliken's population analysis[25] as reported in Ref. 26. This bond charge is found to be $0.4e$, a substantial value compared with the bond charge of $0.5e$ for bulk silicon.[26] This confirms that the two adatoms are chemically bonded, i.e., they are indeed dimers (referred as *C* dimer hereafter).

We next address the issue why *C* dimers appear dark in the filled-state and bright in the empty-state images of STM.[5–7] Since the brightness of the STM image is directly related to the local electronic density of states (LDOS), we calculated the LDOS at the location of the *C* dimer. In Fig. 2, the LDOS of an isolated *C* dimer is shown as a function of energy. It can be seen that the LDOS for the *C* dimer at and below the Fermi energy (~-6.9 eV) is very small, whereas there is a broad pronounced peak above the Fermi energy that is centered around -4.9 eV. Hence, the *C* dimer will appear dark in the filled-state and very bright in the empty-state STM images.[5]

To further understand the nature of the pronounced peak above the Fermi energy, we have performed a local (i.e., orbital as well as bond) analysis of the electronic structure.[26]

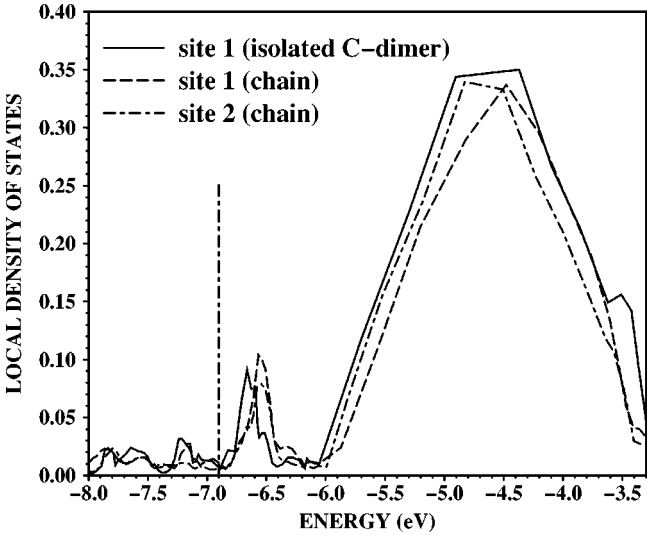

FIG. 2. Local electronic density of states vs energy are shown for site 1 of an isolated *C* dimer (solid line) and sites 1 and 2, respectively, of a *C* dimer in the chain (dashed and dashed-dotted lines). Note that for an isolated *C* dimer, sites 1 and 2 are equivalent. Similarly, for a two-unit chain, sites 1 and 2 are equivalent to sites 6 and 4, respectively. The vertical dashed-dotted line indicates the location of the Fermi level (~ -6.9 eV).

We found that the peak in the LDOS for the *C* dimer oriented along the *x* direction has contributions mainly from p_y and p_z orbitals, with the contribution from p_x orbital amounting to less than 10%. In other words, an adatom in the *C* dimer has little influence on the LDOS of the other adatom. Because of this feature, the brightness of the *C* dimer in STM images will be similar to that of a monomer. Furthermore, we found that the eigenstates contributing to the peak have antibonding characteristics arising mainly from (a) the antibonding between atoms 1 and 2 of the *C* dimer, and (b) the antibonding between one of the atoms of the *C* dimer and its two nearest-neighbor substrate atoms. We have also found that there are no surface states due to the clean $c4\times2$ surface in the energy range of the pronounced peak.

Having established the structure and nature of the *C* dimer, we next consider the formation of larger adatom structures, in particular, the chain structure and the dilute-dimer row. As a first step towards studying larger growth structures, we examine in detail the possible three-adatom structures. Using the *C* dimer as seed, we place the third adatom at a site marked either 3, 4, or 5 (see Fig. 1) and allow the entire system to relax (except the fixed layers at the bottom) using the $O(N)$/NOTB-MD. For this relaxed system, we calculate the binding energies corresponding to each of the three-adatom configurations. Denoting $E_b(i)$ as the binding energy of a three-adatom configuration with the *C* dimer at sites 1 and 2 and the third atom at site i ($i=3,4$, or 5), E_{atom} as the energy of an isolated atom in vacuum, and E_{sys} the energy of the slab with three-adatoms adsorbed, we have $E_b(i)=E_{slab}+3E_{atom}-E_{sys}$. Using $E_b(5)$ as reference, we obtain $E_b(3)=0.65$ eV, $E_b(4)=0.15$ eV, and $E_b(5)=0$ eV, respectively. Since site 3 has the highest binding energy, this will favor the formation of three adatom clusters at sites 1, 2, and 3, respectively, and hence would promote the growth of a diluted-dimer-row rather than a chain structure.

It is then puzzling how a chain structure as reported in experiments[5,6] can be formed. Could it be that these structures are kinetically favorable although they are not energetically favorable? To find the answer to this question, we calculated the barriers to diffusion between sites. In these calculations, only the *y* component of the position coordinate of the third adatom is held fixed for each sampling point (separated by an interval of 0.1 Å) along a diffusion path, while the other two components as well as the coordinates of the rest of the atoms in the system are fully relaxed. This calculation yields the diffusion barriers between sites 3, 4, and 5 as follows: $E(5\rightarrow4)=0.78$ eV, $E(4\rightarrow5)=0.93$ eV, and $E(4\rightarrow3)=1.03$ eV. Assuming that the diffusion rate has an exponential dependence on the energy barrier, i.e., $K(i\rightarrow j)\sim e^{-E(i\rightarrow j)/k_BT}$, one can estimate the relative rates of diffusion between these sites at room temperature as: $K(4\rightarrow5)/K(5\rightarrow4)=3\times10^{-3}$ and $K(4\rightarrow3)/K(5\rightarrow4)=5\times10^{-5}$. Thus, it is relatively easy for the third adatom to reach site 4 from site 5, but it is much harder for it to move from site 4 to site 3 (the lowest energy site). In fact, the third adatom will be trapped at site 4 for a period of time that depends sensitively on the temperature. If the temperature is not high enough, the third adatom at site 4 will have enough time to wait for a fourth adatom to arrive at site 6. This will lead to the formation of two units of the chain structure. If one defines τ_r to be the average resident time for the third adatom at site 4, τ_a the average arrival time of a fourth adatom at site 6, one would have $\tau_r>\tau_a$ for the formation of a chain structure and $\tau_r<\tau_a$ for the formation of a diluted-dimer-row. As temperature increases, τ_r decreases (the third adatom can more easily reach site 3) and hence the formation of a diluted-dimer-row will be favored over that of a chain structure. This analysis clearly suggests that the competition between kinetics and thermodynamics eventually dictates the type of large adatom structures found on Si(100). The results of our analysis is also consistent with the experimental findings.[5,6] It is also interesting to note that since τ_a decreases with the increase of deposition flux, rapid deposition of adatoms will favor the formation of chain structures. However, the effect of deposition flux on the formation of chain structures has not yet been explored experimentally.

We have also performed MD simulations of the two-unit chain structure with adatoms at sites 1, 2, 4, and 6, respectively (see Fig. 1). We found that indeed this two-unit chain structure is a local energy minimum configuration. We estimated the difference of the adsorption energy of a four-adatom chain and that of two isolated *C* dimers to be approximately 0.2 eV. The bond length of the *C* dimer in the chain structure is found to be the same as that of an isolated *C* dimer. We have also calculated the LDOS at the sites of the chain structure and they are shown in Fig. 2. The overall feature of the LDOS is almost the same as that of an isolated *C* dimer, namely, the LDOS is very small at the Fermi energy and has a very broad peak above the Fermi energy. Therefore, the chain structure, just as in the case of *C* dimers, will appear dark in the filled state STM images and bright in the empty state ones.[5]

Finally, we would like to *rationalize* why the chain structure grows in a specific direction. To understand this, recall

that the adjacent dimer rows of the clean $c4\times2$ surface of Si(100) are correlated in an ''antiferromagnetic manner'' both along and perpendicular to the dimer rows. The presence of a *C* dimer, however, breaks the symmetry of the $c4\times2$ surface, creating two faulted channels (shown as shaded areas in Fig. 1). In a faulted channel, the dimers in the adjacent rows are buckled in the ''ferromagnetic'' configuration. Such an arrangement of the dimers is frustrated. This frustration can be eliminated when a diffusing adatom flips the orientation of the buckling so as to restore the arrangement to the ''antiferromagnetic'' order which is the favored configuration. Therefore, we believe that an adatom may diffuse faster on top of the faulted dimer rows as compared to the unfaulted ones, as in the latter case the flipping tends to induce frustration. This facilitates the attachment of the adatoms to the *C* dimer at location 4 and 6 and the formation of two units of the chain structure (''1–2'' and ''4–6''). On the other hand, for an adatom diffusing on the unfaulted dimer rows, i.e., those adatoms approaching the *C* dimer from below, there is no additional mechanism coming into play to lower the energy or favor its attachment to the mirror site $4'$. As a result, the chain structure will grow in the faulted upper half plane in a specific direction as shown in Fig. 1. Note that once a two unit structure is formed, the faulted channel will move to the right by one surface unit. Continuation of the attachment of new adatoms will result in the formation of a larger chain structure. The same argument applies to the formation of the chain structure to the left of the *C* dimer. The presence of both left and right faulted regions will eventually lead to the formation of a V-shaped structure as observed in Ref. 5.

This work was supported by the following agencies and grants: NSF (DMR-9802274 and EPS-9452895), Research Corporation (Cottrell College of Science Grant), University of Louisville (IRIG), and Oak Ridge National Laboratory managed by Lockheed Martin Energy Research Corporation for the Department of Energy under Contract No. DE-AC05-96OR22464.

[1] Y.W. Mo and M.G. Lagally, Surf. Sci. **248**, 313 (1991); **268**, 275 (1992).
[2] R.A. Wolkow, Phys. Rev. Lett. **74**, 4448 (1995).
[3] P.J. Bedrossian, Phys. Rev. Lett. **74**, 3648 (1995).
[4] Z. Zhang, F. Wu, H.J.W. Zandvliet, B. Poelsema, H. Metiu, and M.G. Lagally, Phys. Rev. Lett. **74**, 3644 (1995).
[5] J. van Wingerden, A. Van Dam, M.J. Haye, P.M.L.O. Scholte, and F. Tuinstra, Phys. Rev. B **55**, 4723 (1997).
[6] X.R. Qin and M.G. Lagally, Science **278**, 1444 (1997).
[7] W. Wulfhekel, B.J. Hattink, H.J.W. Zandvliet, G. Rosenfeld, and B. Poelsema, Phys. Rev. Lett. **79**, 2494 (1997).
[8] Y.W. Mo, J. Kleiner, M.B. Webb, and M.G. Lagally, Phys. Rev. Lett. **66**, 1998 (1991).
[9] C.Z. Wang, C.T. Chan, and K.M. Ho, Phys. Rev. B **39**, 8586 (1989).
[10] Gun-Do Lee, C.Z. Wang, Z.Y. Lu, and K.M. Ho, Phys. Rev. Lett. **81**, 5872 (1999).
[11] C.S. Jayanthi, S.Y. Wu, J. Cocks, N.S. Luo, Z.L. Xie, M. Menon, and G. Yang, Phys. Rev. B **57**, 3799 (1998).
[12] M. Menon and K.R. Subbaswamy, Phys. Rev. B **55**, 9231 (1997).
[13] J. Dabrowski and M. Scheffeler, Appl. Surf. Sci. **56**, 15 (1992).
[14] J.E. Northrup, Phys. Rev. B **47**, 10 032 (1993).
[15] V. Milman, S.J. Pennycook, and D.E. Jesson, Thin Solid Films **272**, 375 (1996).
[16] R.M. Tromp, R.G. Scmeenk, F.W. Saris, and D.J. Chadi, Surf. Sci. **133**, 137 (1983).
[17] C.M. Wei, H. Huang, S.Y. Tong, G.D.S. Glander, and M.B. Webb, Phys. Rev. B **42**, 11 284 (1990).
[18] P.S. Mangat, P. Soukiassian, K.M. Schirm, L. Spiess, S.P. Tang, A.J. Freeman, Z. Hurych, and B. Delley, Phys. Rev. B **47**, 16 311 (1993).
[19] G.K. Wertheim, D.M. Riffe, J.E. Rowe, and P.H. Citrin, Phys. Rev. Lett. **67**, 120 (1991).
[20] Yufeng Zhao (private communication).
[21] A.P. Smith, J.K. Wiggs, H. Jonsson, H. Yan, L.R. Corrales, P. Nachtigall, and K.D. Jordan, J. Chem. Phys. **102**, 1044 (1994).
[22] V. Milman, D.E. Jesson, S.J. Pennycook, M.C. Payne, M.H. Lee, and I. Stich, Phys. Rev. B **50**, 2663 (1994).
[23] G. Brocks, P.J. Kelly, and R. Car, Phys. Rev. Lett. **66**, 1729 (1991).
[24] K. Terakura, T. Yamasaki, T. Uda, and I. Stich, Surf. Sci. **386**, 207 (1997).
[25] R.S. Mulliken, J. Chem. Phys. **23**, 1833 (1955).
[26] D.R. Alfonso, Shi-Yu Wu, C.S. Jayanthi, and E. Kaxiras, Phys. Rev. B **59**, 7745 (1999).